行政院國家科學委員會補助專題研究計畫　V 成果報告

在四族半導體表面上的超薄離子固體自我組裝與其薄膜、介面性質

計畫類別：V 個別型計畫　□整合型計畫
計畫編號：NSC 95-2112-M-007-067-MY4
執行期間： 95 年 8 月 1 日至 99 年 7 月 31 日

執行機構及系所：清華大學物理系

計畫主持人：林登松　教授
共同主持人：
計畫參與人員：謝明峰、鐘仁陽、張展源、羅中廷、李宏道、吳欣樺、吳曉穎、黃世鑫

成果報告類型(依經費核定清單規定繳交)：□精簡報告　V 完整報告

本計畫除繳交成果報告外，另須繳交以下出國心得報告：
□赴國外出差或研習心得報告
□赴大陸地區出差或研習心得報告
V 出席國際學術會議心得報告
□國際合作研究計畫國外研究報告

處理方式：除列管計畫及下列情形者外，得立即公開查詢
□涉及專利或其他智慧財產權，□一年□二年後可公開查詢

中　華　民　國 99 年 10 月 11 日

國科會補助專題研究計畫成果報告自評表

請就研究內容與原計畫相符程度、達成預期目標情況作一綜合評估

V 達成目標

未達成目標（請說明，以 100 字為限）

實驗失敗

因故實驗中斷

其他原因

研究成果在學術期刊發表或申請專利等情形：

論文：V 已發表 □未發表之文稿 V 撰寫中 □無

專利：□已獲得 □申請中 □無

技轉：□已技轉 □洽談中 □無

其他：(以 100 字為限)

請依學術成就、技術創新、社會影響等方面，評估研究成果之學術或應用價值(簡要敘述成果所代表之意義、價值、影響或進一步發展之可能性)（以 500 字為限）

The nature of solid-solid interface bonding is a topic of great scientific interest and a key issue pertaining to the functionality of solid state devices made of thin films. The chemical character of the interface bonding is generally firmly established at the very early stages of film growth (in which the first one or two atomic layers are grown). One of the most surprising discovery we made is that the bonding character at the interface between NaCl and Ge switches periodically between ionic bonding and van der Waals bonding during layer-by-layer growth of NaCl on Ge. As a result, all of the cation and anion core level binding energies shift in unison by about 1.7 eV, a huge effect in terms of charge transfer and polarization switch at the interface. This finding is unprecedented and is made possible in the present work by employing half reactions. In other words, the NaCl films were built up by alternately depositing Cl and Na, as opposed to the usual MBE growth involving the deposition of ionically neutral alkali halides.

We believe that the work in highly relevant to the fundamental physics of surfaces, interfaces, and thin films. Our discovery has strong implications regarding the synthesis and properties of nanomaterials and devices containing ionic-covalent junctions, such as high-*k* materials on silicon.

結果簡要說明

過去四年，我們對超薄離子固體累積更多更好瞭解，其中很值得在此一提的是，我們發現: 離子固體薄膜表面上的化學反應居然可以穿越數個原子層厚的薄膜，迫使薄膜與基版間的原子與電子結構產生具大的改變，也就是薄膜與基版間產生了電壓差為 1.6-eV 左右的電雙極層，這種由表面引發的介面電子組態的重整是史無前例的，我們相信對表面、介面、與薄膜研究社群會有不小的衝擊。這個結果"Electronic Reconstruction at a buried ionic-covalent interface driven by surface reactions"其實應該可以在很所謂高衝擊系數的期刊登出，最後可惜只在 Phys. Rev. 發表。另外，我們也將最典型的離子固體/共價鍵半導體界面系統，以實空間原子影像、同步輻射光電子譜、第一原理模擬計算等綜合、完整地研究完成、因此，我們相信這也是一篇很有價值的成果與科學發現。本篇報告"Sodium chloride nano-films on Si(100) grown by molecular beam epitaxy" 也已投稿審查中，稿件附於後。

我們在計畫中，對每一個研究，我們通常綜合應用實驗室自有的電子穿隧效應顯微鏡、同步輻射光電子譜、量子計算模擬、蒙地卡羅模擬等互補技術加以分析探討，以求其完整。過去四年成果，我們擇其重要者說明如下。

1. Possibility of direct exchange diffusion of hydrogen on the Cl/Si(100)-2×1 surface, Physical Review B **80**, 045304 (2009). 原子直接交換式擴散現象是很多凝態物理、薄膜物理、表面物理等教科書中的會談到的標準擴散模型，但也常會提到種擴散現象因其高能量過程而只在高溫發生。我們以顯微鏡影片顯影與測量(極可能的)的原子直接交換式擴散現象，我們也融合理論模擬，說明其發生的可能中間態過程與原因。

2. C.-T. Lou, H.-D. Li, J.-Y. Chung, D.-S. Lin*, T.C. Chiang*, Oscillations of Bond Character and Polarization at the NaCl/Ge(100) Interface during Cyclic Growth, Physical Review B (Condensed Matter and Materials Physics) **80**, 195311 (2009). 發生於奈米薄膜表面上的物理化學反應，竟會穿越數個原子層厚薄膜而引起薄膜與基板間介面的電子組態構造強烈變化?我們以同步輻射光電子譜說明這在離子固體薄膜上是常會發生的。

3. Mediation of Chain Reactions by Propagating Radicals during Halogenation of H-Masked Si(100): Implications for Atomic-Scale Lithography and Processing, J. Chem. Phys. **130**, 1 (2009). 我們(應是首次)以實空間原子影像觀測與證實一個活性原子可以在表面上引起連鎖反應，我們也定量得出活性原子擴散方位、距離與其引發連鎖反應的次數。

4. Correlation of Reaction Sites during the Chlorine Extraction by Hydrogen atoms from Cl/Si(100)-2*x*1, J. Chem. Phys. **127**, 034708 (2007).氣體分子撞擊晶體表面而產生化學反應時，其反應當然是在該撞擊點發生嗎?我們以實空間原子影像、同步輻射光電子譜、蒙地卡羅模擬計算等綜合研究，證明這種直覺性的想法不是全然正確的，反應是在該撞擊點周邊不遠的區域內發生。

5. Atomistic View of the Recombinative Desorption of H2 from H/Si(100), Phys. Rev. Lett. 94, 196103 (2005).我們以高解析度實空間原子影像直接觀測一個重要的化學物理現象: 氫重組合分子熱脫附反應與其發生的兩段式表面原子排列重組過程機制。

Report on Sodium chloride nano-films on Si(100) grown by molecular beam epitaxy

Abstract

Sodium chloride (NaCl) films were grown on an Si(100)-(2 × 1) surface at near room temperature by molecular beam epitaxy (MBE). The atomic structure and growth mode of the prototypical ionic materials on the covalent bonded semiconductor surface is examined by synchrotron core-level X-ray photoemission spectrum (XPS), scanning tunneling microscopy (STM), and first-principles calculations. The Si 2*p*, Na 2*p*, and Cl 2*p* core level spectra together indicate that adsorbed NaCl molecules at submonolayer coverage (i.e., below 0.4 monolayer (ML)) partially dissociate and form Si-Cl species, and that a significant portion of the dangling bond characteristics of the clean surface remain after NaCl deposition of a 1.8 ML. The deposition of 0.65 ML NaCl forms a partially ordered adlayer, which includes NaCl networks, Si-Cl species, adsorbed Na species, and isolated dangling bonds. The STM results revealed that the first adlayer consists of bright protrusions which form small c(2 × 4) and (2 × 2) patches. Above 0.65 ML, the two dimensional NaCl double-layer growth proceeds on top of the first adlayer.

PACS Numbers: 68.55.J-, 77.55.Px, 68.43.-Hn, 68.37.Ef

1. Introduction

The epitaxial growth of insulating nano-films on semiconductor surfaces has attracted much attention due to potential applications in microelectronic and optoelectronic devices, and has aroused scientific interest in the basic principles of epitaxial growth and heterostructure physics.[1-3] NaCl is a prototypical insulator with a large percentage of ionic character. The Si(100) wafers are most commonly used in making Si-based devices and much is known about their surface atomic and electronic structures. Therefore, NaCl/Si(100) can be used as a model system for studying the interfacial properties and growth behavior between ionic crystals and a covalent substrate.

Previous studies have established that, under suitable conditions, NaCl can be grown lattice-matched to Ge(100) with a high degree of quality.[4-7] An STM measurement suggests that the growth of NaCl begins with a carpet-like double-layer of NaCl film.[5] In an electron energy loss scattering (EELS) measurement, Zielasek, Hildebrandt and Henzler found electronic states at the NaCl/Ge interface and suggested that the dimerization of the Ge(100) surface is not eliminated at the NaCl/interface - even if the thickness of the NaCl rises to 20 ML.[6] Growth mode of the NaCl/Si(100) system has been less-well studied, perhaps due to the lattice mismatch. The second-nearest-neighbor separation R_1 for a NaCl crystal is 3.98 Å. The surface lattice constant *a*, or the period of unreconstructed Si(100)-1×1, is 3.84 Å. The lattice mismatch at the heterostructure of NaCl/Si(100) is close to 4%.

Given a large lattice mismatch, the growth of alkali halide on the Si and Ge surfaces at sub-monolayer coverage does not yield an ordered surface structure. For example, LiBr (R_1=3.89 Å) and LiF (R_1 = 2.85Å) are adsorbed randomly onto Si(100) at room temperature. KI (nearest-neighbor separation R_0 = 3.53 Å) dissociatively adsorbs on the Si(100) surface at a coverage of less than 0.5 ML.[8] Although thick flat films can be obtained, the growth of KI, LiF and LiBr on Si(100) and Si(111) surfaces proceeds by the Volmer-Weber (VW) mechanism of island growth as a result of the interfacial lattice mismatch.[8-10] However, Tsay *et al.* found that KCl can grow on Si(100) in a layer-by-layer fashion.[11]

In the present work, NaCl nano-films were grown by means of MBE and the resulting films were examined *in situ* by high resolution synchrotron radiation photoemission and STM. *Ab initio* calculations were also applied to model the atomic structure of the first adlayer. Compared to LiF/Si(100) and KCl/Si(100) systems, NaCl/Si(100) has a smaller lattice misfit. Experimental results reveal an unusual growth mode: an adlayer consisting of about 0.65 adsorbed NaCl is formed, followed by a double-layer growth. The first adlayer consists mainly of an NaCl network and unreacted single dangling bonds that form several types of local ordering. These findings demonstrate the richness of growth modes for even relatively simple ionic crystal/covalent crystal hetero-epitaxial systems.

2. Experimental details

A single crystal Si(100) of 1 × 10 or 3 × 10 mm^2 was sliced from an antimony doped wafer with a

resistivity of 0.01 Ω • cm. The clean Si(100) surface was obtained *in situ* by direct heating to 1450 K for a few seconds after degassing at 900 K for 20 hours. NaCl powder of 99.99% purity was evaporated from an alumina crucible by a feedback current flux-controlled electron bombardment beam. The deposition rate was measured by a quartz-crystal thickness monitor. The coverage of NaCl in ML (denoted by θ), was calculated from the exposure time, assuming the sticking coefficient to be 1. The coverage of 1.0 ML refers to the number of Si atoms on an ideal unreconstructed Si(100) surface with an atomic density of 6.8×10^{14} cm^{-2}. The substrate temperature during growth was approximately 330 K.

The photoemission spectra were recorded in a separated μ-metal-shielded chamber with a based pressure of ~ 3×10^{-10} torr at the Taiwan Light Source Laboratory in Hsinchu, Taiwan. Synchrotron radiation from a 1.5 GeV storage ring was dispersed by a wide-range spherical grating monochromator (SGM). The photocurrent from a gold mesh placed in the synchrotron beam path was monitored to determine the relative incident photon beam flux. Photoelectrons were collected from 45° off normal emission and analyzed by a 125-mm hemispherical analyzer. The overall energy resolution was less than 120 meV. The STM measurement was taken in a separated UHV chamber with a base pressure of 8×10^{-11} torr. The tunneling current I_t was about 0.1 nA. The topographic height measurement did not strongly depend on the sample bias V_s around -2.4 V typically used.

3. Results and discussion

A. Photoemission results

High-resolution X-ray photoemission spectroscopy can be performed to distinguish between atoms at nonequivalent sites and in different chemical bonding configurations, based on shifts in the atoms' binding energies.[12] Figs. 1, 2(a), and 2(b) respectively present a series of surface-sensitive Si 2*p*, Cl 2*p*, and Na 2*p* core-level spectra for the Si(100)-(2 × 1) surface with various amounts of NaCl deposition. Identical Voigt line shapes, each consisting of a pair of spin-orbit split doublets, were used to decompose the Si 2*p* and Cl 2*p* core level spectra into overlapping components (curves). The solid curves represent the fitting results that overlap the data points. Spectra of the chlorine terminated Si(100)-(2 × 1) (Cl/Si(100)) (bottom, Fig. 1) are also presented for reference. The spectrum has two components, B and Si^+, which are separated by 0.90 eV. The B component was responsible for the emission from the bulk atoms and the Si^+ component was responsible from the nominal 1.0 ML of the surface Si-Cl species.[13] The corresponding Cl 2*p* spectrum for Cl/Si(100) (bottom, Fig. 2(a)) can only be analyzed in terms of a single component that has a pair of split doublets separated by 1.60 eV, implying that all Cl has the same Si-Cl monochloride bonding configuration.

Prior to NaCl deposition, the Si 2*p* spectrum (second from bottom, Fig. 1), which was obtained from the clean Si(100)-(2 × 1) surface, has a component (B) and two components S and S', respectively shifted by -0.52 eV and +0.23 eV. The components B and S have been attributed, respectively, to emission from the bulk atoms and the up atoms of asymmetric dimers. The origin of the *S*' component is not clear, but its energy position is consistent with atoms from the subsurface layers.[14, 15] All

core-level binding energies are referenced to the bulk Si $2p_{3/2}$ position (99.5 eV) relative to the valence band maximum.

Figure 1 shows that the intensity of the *S* component in the Si 2*p* spectra declines with increasing NaCl coverage, suggesting a reduction of bare dimers. At $\theta \geq 0.4$ ML, a component on the higher binding energy side can be located near the position of the Si^+ component. This signature suggests that a portion of the deposited NaCl molecules decompose and Si-Cl bonds are present on the surface. Also, the Si 2*p* spectra become broader, as evidenced by the filling of the two spin-orbital split peaks. Thus two additional components, *C* and *I*, are also included in our fittings and the intensities of the *S, I, C* components are displayed in Fig. 3. The coverages (amounts of atoms) that are responsible for both the I and C components, in ML are calculated by comparing their intensity ratios to I_B with I_{Si+}/I_B, assuming I_{Si+} correspond to 1.0 ML of Si-Cl species. The coverage of *S* is similarly calculated by assuming that the S component of the clean Si(100)-(2 × 1) surface corresponds to 0.5 ML of up atoms in bare dimers. The *I* component exhibits a shift of +0.42 eV toward the higher binding energy side. Its coverage also rises with θ up to 0.38 ML at θ = 0.6 ML, but remains largely constant above 0.6 ML. As will be discussed in Sec. 3C, the *I* component is responsible for the Si atoms that are weakly bonded to NaCl clusters.

The fitting results show that the *C* component is shifted from B by +0.90 eV, a value identical to that of the Si^+ peak. Since a large shift commonly results from a large charge transfer, the *C* component is apparently responsible for the Si-Cl surface species. Accordingly, a fraction of the adsorbed NaCl molecule dissociates. The dissociation energy for the ionic NaCl bond in this molecule is 4.3 eV. The Si-Cl bond energy is -3.94 eV. Calculated adsorption energies for Na adatom on Si(100)-(2 × 1) surface is about −2.2 eV.[16] Therefore, it is energetically favorable for an adsorbed NaCl molecule to dissociate. The intensity of the C component or, equivalently, the amount of Si-Cl species or the amount of dissociated NaCl molecules, quickly reaches 0.23 ML at θ = 0.4 ML. It remains rather constant up to θ = 1.8 ML, while those of Na 2*p* and Cl 2*p* keep increasing with the coverage. These observations suggest that the adsorbed NaCl molecules have a higher probability of dissociating at low coverage, when the dangling bond pairs (DBPs) are plentiful.

B. STM results

The initial clean Si(100) surface shows an apparent (2 × 1) reconstruction consisting of parallel rows of dimers. Each surface Si atom has one dangling bond. On the vicinal Si(100) surface, two different types of 0.15 nm high single-height steps, S_A and S_B, separate perpendicular domains of (2 × 1) reconstruction.[17] At the S_A step edges, the direction of the dimer rows on the upper terrace is oriented parallel to the step edge, and perpendicular to the S_B steps. Figure 4 shows a filled-state topographic image for a Si(100) surface after 0.1-ML NaCl deposition at room temperature. Given a very small amount of coverage, the image is often fuzzy, perhaps due to the presence of surface mobile species (dissociated Na). An NaCl adsorbed site appears dimmer than the bare dimers and often occupies only one side of the dimer. The other end of the dimer appears less affected and has about the same apparent height as the bare dimers. Taking the presence of the S component in the Si 2*p* spectra into consideration, the unaffected end is likely a single dangling bond (SDB) on a dimer. As Fig. 4 depicts,

the SDBs can cluster together, suggesting an ample mobility of the impinging NaCl molecules before adsorption.

Figure 5 shows the evolution of the Si(100) surface after various amounts of NaCl deposition at room temperature. Line profiles, each respectively showing a typical topographic height along the line segment in Figs. 5(a), 5(b), 5(c), and 5(d), are presented in Figs. 6(a), 6(b), 6(c), and 6(d). As shown in Fig. 5(a), with increasing NaCl coverage, many (~ 0.35-ML) SDBs are visible as bright protrusions after 0.65-ML NaCl deposition. The 0.65-ML NaCl adsorbed species attach preferentially to surface sites and result in a smooth and fully-formed layer, referred to below as the first adlayer. No islands are observed at this stage, again suggesting that the adsorbed NaCl species is mobile until a stable adsorption site is found. A zoom-in image (Fig. 7(a)) reveals that most bright protrusions resemble SDBs and that few (0.02 ML) DBPs are present. Small dark areas with missing bright protrusions (SDBs) accounting for about 0.1 ML are assigned as dichloride dimer species, owing to the presence of the Si^{+} component in the Si 2*p* spectra (Fig. 1). Many SDBs form small patches with locally-ordered (2 × 2)-A (Figs. 7(b, c)), (2 × 4) (Figs. 7(d, e)), and (2 × 2)-B (Figs. 7(f, g)) structures. The fractional areas with these ordered structures are summarized as percentages in Table I. More detailed atomic models, including other surface species for these structures, are presented in Sec. 3C.

Further deposition on the first adlayer leads to the growth of 2D islands, as shown in Fig. 5(b). In the other words, the first adlayer acts like a wetting layer before further growth. In Sec. 3A photoemission data suggest no further NaCl dissociation above 0.4 ML. Thus, the observed 2D patches are NaCl islands; further-adsorbed NaCl molecules migrate on the first adlayer and nucleate into two-dimensional islands. Steps, especially S_A steps, are good island nucleation sites as many islands are attached to steps in Fig. 5(b). As the coverage increases, the 2D islands grow in size and coalesce into large islands, as Figs. 5(c) and 5(d) exhibit. The corresponding line profiles (Figs. 6(b) and 6(c)) show that the 2D islands have an apparent height of about 3.8 Å above the first adlayer. This value, in between one and two intra-layer Na–Cl distances (2.8 Å and 5.6 Å) of the NaCl crystal, is about the same as that measured on a double-layer island on Ge(100).[5] The measured apparent height is not sensitive to the sample bias voltage of around -2.5 ± 0.3 V. As depicted in Fig. 8, a well-resolved square lattice with a lattice constant of ~3.8 Å is observed on top of the 2D islands in Fig. 5(c). This lattice constant is close to the nearest Cl-Cl distance on a NaCl(100) surface. This observation provides further evidence that the 2D islands are indeed NaCl films of double layer height. Assuming that the 2D islands rest on the first adlayer without removing or adding materials from underneath, the island coverages of 0.18 and 0.50 ML extracted from Figs. 5(b) and 5(c), respectively, account only about one half of the additional deposition above 0.65 ML. Together, these considerations indicate that those 2D islands are NaCl double-layers. Although similarly observed on Ge(100), the double layer in Figs. 5(b) and 5(c) rests on the first adlayer, as opposed to resting directly on the lattice matched Ge(100) surface. It appears that the first adlayer serves to damp out the strain due to lattice misfit between the NaCl and Si interface.

C. Atomic model for the first adlayer

We now discuss the atomic structure of the local ordering in the first adlayer upon the deposition of 0.65 ML of NaCl. At this coverage, STM images and the S component in the Si 2*p* spectra indicate that

about 0.35-ML of SDBs are present on the surface. Based on the total NaCl coverage and the ordered arrangement of SDBs in Fig. 5, we placed NaCl molecules on top of the clean Si(100) surface, and performed density functional calculations to determine the relaxed structure and relevant total energy. Prior to relaxation, the initial NaCl molecules were placed 45° with respect to the dimer bond direction with Na ions either near pedestal sites or cave sites. The atomic structures after relaxation are summarized in Fig. 9 and 10. The calculations were based on the Vienna *ab initio* simulation program (VASP) using the projector-augmented wave method and the revised Perdew-Burke-Ernzerhof pseudopotential.[18, 19] The Si substrate was modeled by a $4 \times 4 \times 8$ slab, with its bottom surface terminated by hydrogen. A vacuum region of thickness 11.84 Å on top of the Si surface was included to form a supercell. The irreducible Brillouin zone was sampled with a $(4 \times 4 \times 1)$ Monkhorst-Pack mesh, the energy cutoff was set at 400 eV, and the energy convergence was set at 10^{-4} eV. The bottom four Si layers were held frozen; all other atoms were fully relaxed with the residual atomic forces at less than 0.02 eV/Å. This relaxation allows the system to evolve and find equilibrium.

As shown in Figs. 9 and 10, the buckled dimer structure remained largely intact with a slightly reduced tilt angle. We tried to place NaCl molecules parallel to dimer bonds. The relaxed structure was similar to that found in Ref. ([20]). However, the energy obtained was higher than those shown in Figs. 9 and 10. For (2×2)-A, NaCl had a local coverage of 0.5 ML and formed nominally flat zig-zag chains along the dimer rows. With an increased local NaCl coverage of 0.75 ML, Cl ions, in coherence with the corresponding buckled dimers, tilted up and down in the relaxed (2×4) and (2×2)-B structure (Figs. 10(b) and 10(c)). The NaCl adlayer became rather non-planar, similar to that found in the KCl/Si(100) system. Unfortunately, ionic species have a low state density near the Fermi level, contributing to tunneling currents, and STM images such as those in Figs. 5(a) cannot resolve and are, therefore, unable to verify the detailed atomic registry for Na and Cl ions. Instead, STM images predominately show SDBs which have a finite (nonzero) density of states near the Fermi level. Judging from the flatness of the subsequent NaCl double-layer shown in Figs. 5 and 8, the non-planar structures in Figs. 10(b) and 10(c) likely flatten out by the flip-flop motion of buckled dimers.[21]

4. Conclusions

A new growth mode is found during molecular beam epitaxy of ionic nanofilms on a covalent crystal surface. We studied the adsorption of NaCl on a Si(100)-(2×1) surface at room temperature up to 2.25 ML with synchrotron x-ray core-level photoelectron spectroscopy and scanning tunneling microscopy. As $\theta < 0.4$ ML, the XPS and STM results together indicated that more than half of the adsorbed NaCl dissociates to form Si-Cl and adsorbed Na. A wetting adlayer is formed after the deposition of 0.65 ML NaCl. This adlayer consists of Si-Cl, adsorbed Na, NaCl networks, and isolated dangling bonds. Many isolated dangling bonds are grouped into small patches, which exhibit the (2×4) or (2×2) ordered structure. Further deposition above 0.65 ML results in the appearance of double-layer NaCl islands which grow in size on top of the first adlayer. Up to $\theta = 1.8$ ML, the isolated dangling bonds remain at the interface between the NaCl film and the silicon substrate. With the first adlayer acting as a buffer layer, this system demonstrates that a relaxed film of ionic NaCl solid can be grown on the Si(100) surface despite the 3.6% lattice mismatch.

REFERENCES

1 G. D. Wilk, R. M. Wallace, and J. M. Anthony, J. Appl. Phys. 89, 5243 (2001).

2 S. Silvia and S. Wolf-Dieter, J. Phys.: Condens. Matter 16, R49 (2004).

3 K. Saiki, Appl. Surf. Sci. 113-114, 9 (1997).

4 C. T. Lou, H. D. Li, J. Y. Chung, D. S. Lin, and T. C. Chiang, Phys. Rev. B 80, 195311 (2009).

5 K. Glöckler, M. Sokolowski, A. Soukopp, and E. Umbach, Phys. Rev. B 54, 7705 (1996).

6 V. Zielasek, T. Hildebrandt, and M. Henzler, Phys. Rev. B 69, 205313 (2004).

7 C. A. Lucas, G. C. L. Wong, C. S. Dower, F. J. Lamelas, and P. H. Fuoss, Surf. Sci. 286, 46 (1993).

8 H. Guo and R. Souda, J. Appl. Phys. 92, 6621 (2002).

9 H. Guo, H. Kawanowa, and R. Souda, Appl. Surf. Sci. 158, 159 (2000).

10 M. Katayama, K. Ueno, A. Koma, M. Kiguchi, and K. Saiki, Jpn. J. Appl. Phys., Part 1 43, L203 (2004).

11 S. F. Tsay, J. Y. Chung, M. F. Hsieh, S. S. Ferng, C. T. Lou, and D. S. Lin, Surf. Sci. 603, 419 (2009).

12 F. J. Himpsel, B. S. Meyerson, F. R. Mc Feely, J. F. Morar, A. Taleb-Ibrahimi, and J. A. Yarmoff, in Proceeding of the Enrico Fermi School on "Photoemission and Absorption Spectroscopy of Solids and Interfaces with Synchrotron Radiation", edited by M. Campagna and R. Rosei (North Holland, 1988), p. 203.

13 D. S. Lin, J. L. Wu, S. Y. Pan, and T. C. Chiang, Phys. Rev. Lett. 90, 046102 (2003).

14 P. E. J. Eriksson and R. I. G. Uhrberg, Phys. Rev. B 81, 125443 (2010).

15 H. Koh, J. W. Kim, W. H. Choi, and H. W. Yeom, Phys. Rev. B 67, 073306 (2003).

16 P. Gravila and P. F. Meier, Phys. Rev. B 59, 2449 (1999).

17 B. Voigtländer, T. Weber, P. Å milauer, and D. E. Wolf, Phys. Rev. Lett. 78, 2164 (1997).

18 G. Kresse and J. Furthmüller, Phys. Rev. B 54, 11169 (1996).

19 G. Kresse and J. Hafner, Phys. Rev. B 49, 14251 (1994).

20 A. Maximilian and et al., Nanotechnology 20, 445301 (2009).

21 J. Nakamura and A. Natori, Phys. Rev. B 71, 113303 (2005).

Table I. Measured fractional areas, the NaCl coverage and dangling bond (DB) coverage in model structures for various patterns and surface species.

Pattern/ species	Fractional area (%)	NaCl coverage	DB coverage
Disordered DBs	26	-	-
(2 × 2)-A	26	0.5	0.25
(2 × 4)	16	0.75	0.25
(2 × 2)-B	12	0.75	0.25
Cl-Si-Si-Cl	10	0	0
DBP	2	0	0

FIG. 1. (Color online) Si 2*p* core level photoemission spectra (dots) of Si(100) surface with various amounts of NaCl deposition, as specified. The solid curves fit to the spectra. The curves labeled B, S, I and Si^+ are the results, respectively, of the decomposition of the Si 2*p* spectra into contributions from the bulk, the clean surface, the interface layer and the Si-Cl species. The energy zero refers to the $2p_{3/2}$ bulk position. The dashed lines are guides.

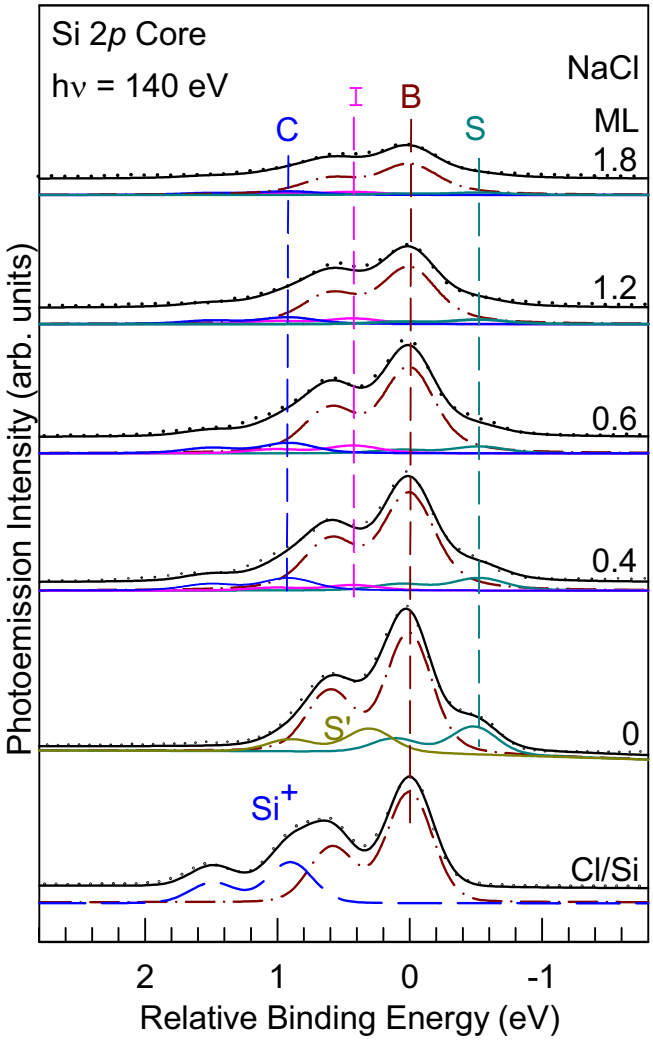

FIG. 2. (Color online) (a) Cl 2*p*, and (b) Na 2*p* core level photoemission spectra (dots) corresponding to Si 2*p* spectra in Fig. 1. The solid curves fit to the spectra. To eliminate the band-bending effect, the relative binding energies refer to the corresponding Si the $2p_{3/2}$ bulk positions in Fig. 1.

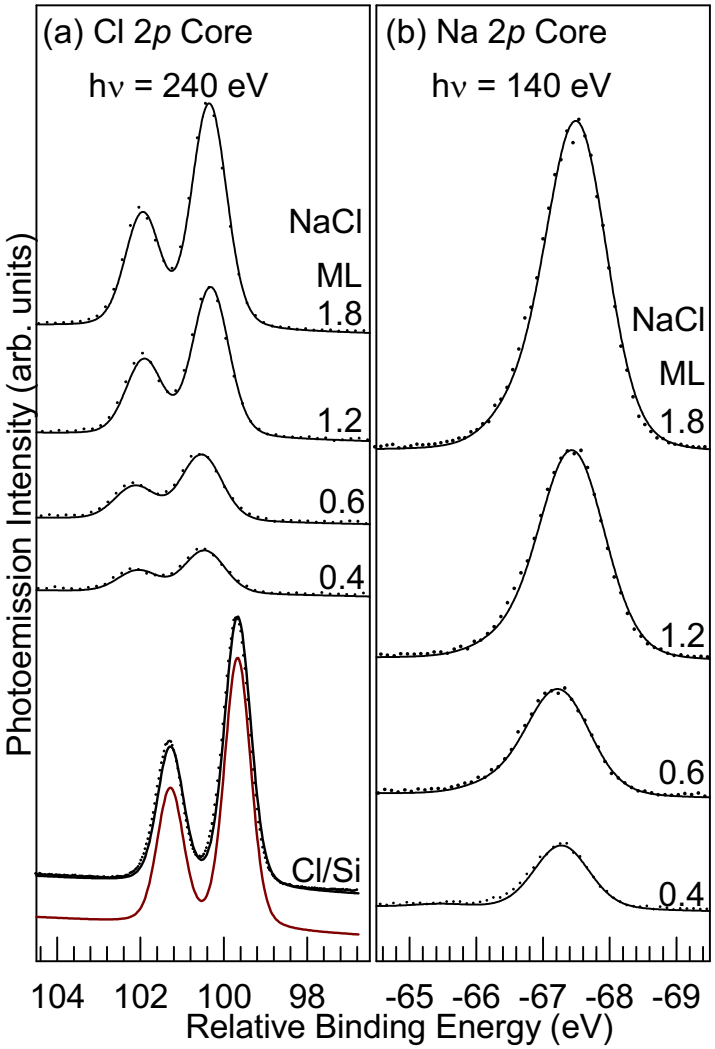

FIG. 3. (a) Coverage evolution of the S, S^+, and I components in the Si 2*p* spectra. (b) Integrated photoemission intensities of Si 2*p*, Cl 2*p*, and Na 2*p* as functions of NaCl coverage.

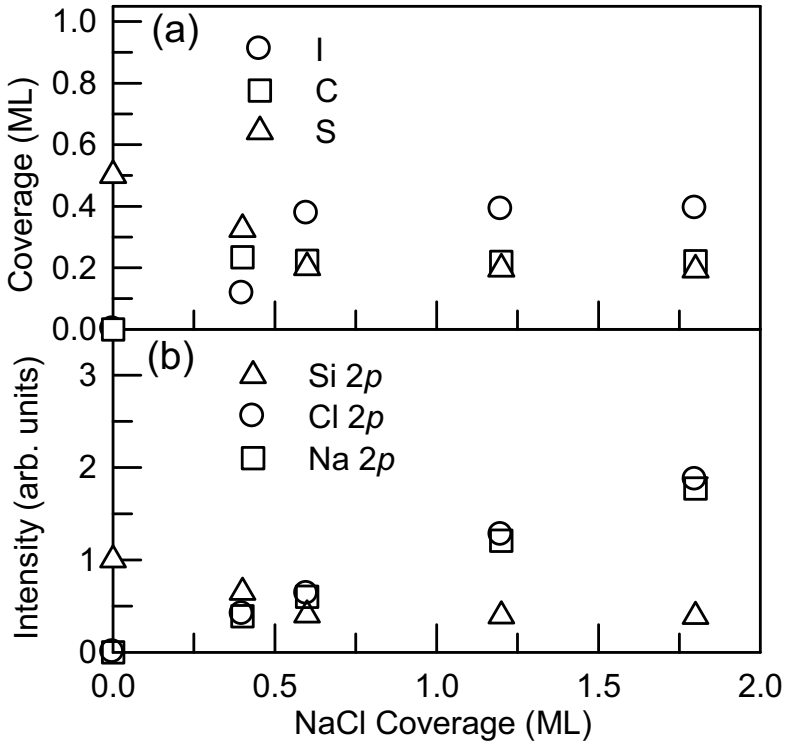

FIG. 4. (Color online) STM images of 0.1 ML NaCl on Si (100) with V_s = -1.8 V. The dimer rows running diagonally can be discerned. The two centered bright protrusions are unknown species. The arrow points to an adsorption site that makes one end of a dimer darker. The white dashed arrow lying along a dimer row direction points to a clustered NaCl adsorption sites.

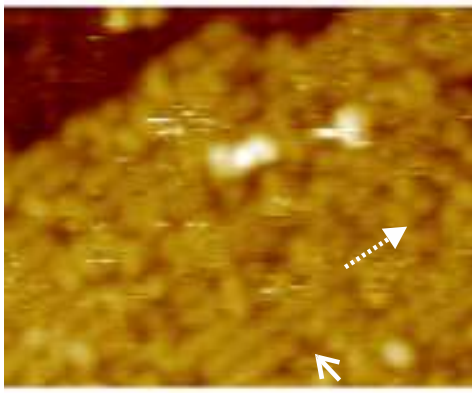

FIG. 5. (Color online) Filled-state STM images showing morphology evolution with various NaCl coverages on Si(100), as labeled. All images are obtained at room temperature with I_t = 0.23 nA and V_s = (a) -2.05, (b) -2.3, (c), and (d) -2.8 V. The images cover an area of about (a) 80 × 40 nm^2, and (b)-(d) 300 × 150 nm^2.

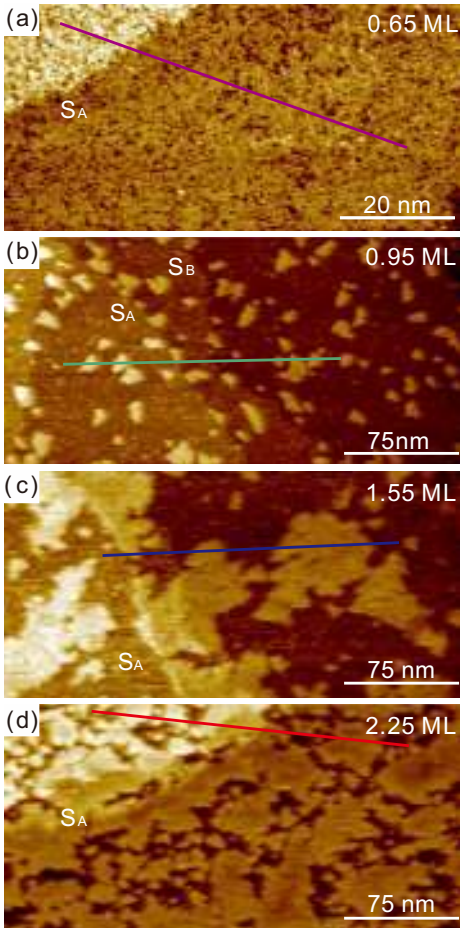

FIG. 6. (Color online) Corresponding apparent topographic height profiles along the line segments in Fig. 5 and schematics of grown NaCl nano-films. The thin yellow layer above the substrate depicts the first adlayer. A thick yellow rectangle indicates an NaCl monolayer.

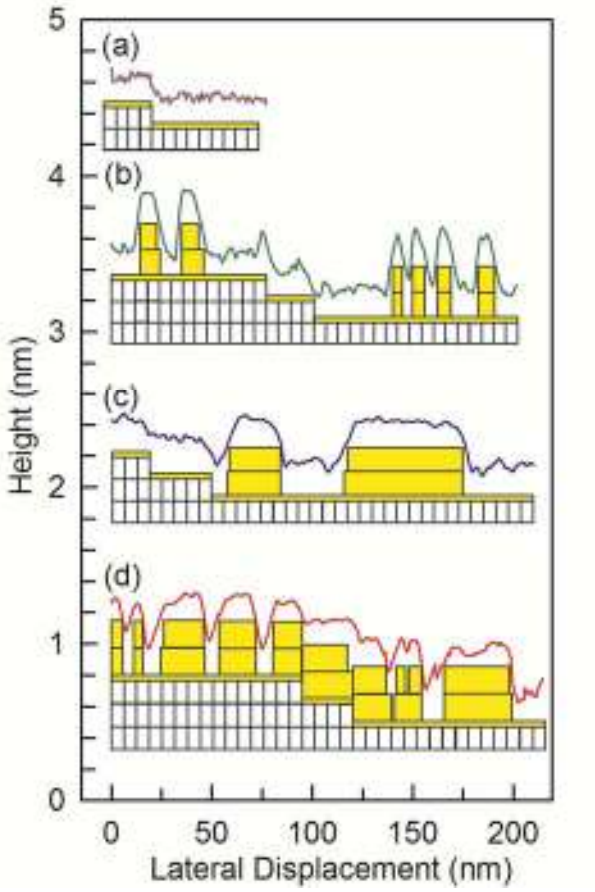

FIG. 7. (Color online) (a) 20.0 × 10.0 nm^2 STM images of Si(100) after deposition of 0.6 ML NaCl. The double arrow indicates the dimer row direction. Sample bias voltage used was -2.05 V. (b, d, f) Zoom-in images and (c, e, g) corresponding schematic diagrams for selective areas on the same sample as that in (a). White rectangles enclose local ordered unit cells as indicated. Yellow circles in (c, e, g) indicate the positions of bright protrusions. Details of the atomic models are shown in Fig. 9.

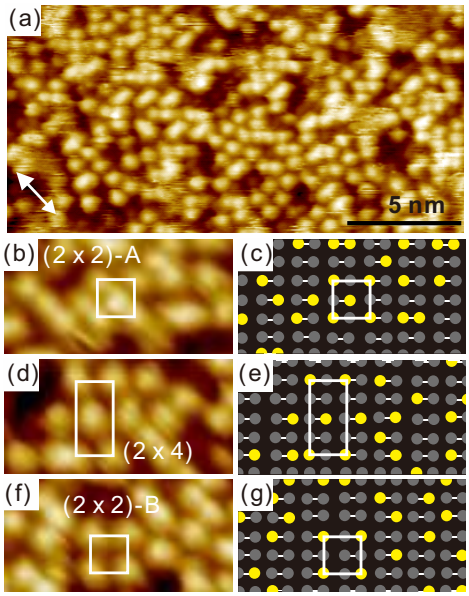

FIG. 8. (Color online) (a) 10 × 5 nm^2 STM image with atomic resolution on top of an isolated island on the same surface as Fig. 5(c). The sample voltage was -2.8 V. The double arrow on the lower left indicates a dimer row direction on the original substrate.

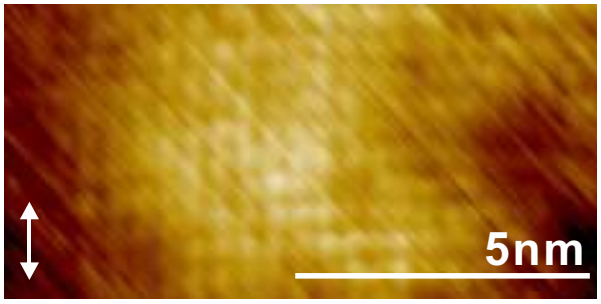

FIG. 9. (Color online) Top views of the relaxed structures for the (a) (2 × 2)-A, (b) (2 × 4), and (c) (2 × 2)-B ordering. The numbers are atom labels. The dotted line rectangles enclose unit cells.

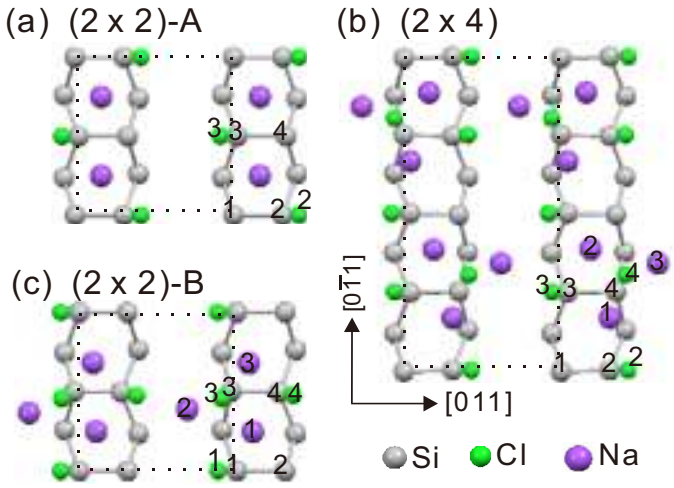

FIG. 10. (Color online) Corresponding side views of the relaxed structures shown in Fig. 9. Distances are given in Angstroms.